Proceedings of IMECE04
2004 ASME International Mechanical Engineering Congress and Exposition
November 13-20, 2004, Anaheim, California USA

IMECE2004-59149

INTERFACE EFFECT ON LATTICE THERMAL CONDUCTIVITIES OF SUPERLATTICE NANOWIRES

Yunfei Chena
Department of Mechanical Engineering and China Education Council Key Laboratory of MEMS, Southeast University, Nanjing, 210096, P. R. of China

Deyu Li
Department of Mechanical Engineering, Vanderbilt University, Nashville TN, 37235-1592

Juekuan Yang
Department of Mechanical Engineering and China Education Council Key Laboratory of MEMS, Southeast University, Nanjing, 210096, P. R. of China

Zhonghua Ni
Department of Mechanical Engineering and China Education Council Key Laboratory of MEMS, Southeast University, Nanjing, 210096, P. R. of China

Jennifer R. Lukes
Department of Mechanical Engineering and Applied Mechanics, University of Pennsylvania, Philadelphia PA 19104-6315

ABSTRACT

The nonequilibrium molecular dynamics (NEMD) method has been used to calculate the lattice thermal conductivities of Ar and Kr/Ar nanostructures in order to study the effects of interface scattering, boundary scattering, and elastic strain on lattice thermal conductivity. Results show that interface scattering poses significant resistance to phonon transport in superlattices and superlattice nanowires. The thermal conductivity of the Kr/Ar superlattice nanowire is only about 1/3 of that for pure Ar nanowires with the same cross sectional area and total length due to the additional interfacial thermal resistance. It is found that nanowire boundary scattering provides significant resistance to phonon transport. As the cross sectional area increases, the nanowire boundary scattering decreases, which leads to increased nanowire thermal conductivity. The ratio of the interfacial thermal resistance to the total effective thermal resistance increases from 30% for the superlattice nanowire to 42% for the superlattice film. Period length is another important factor affecting the effective thermal conductivity of the nanostructures. Increasing the period length will lead to increased acoustic mismatch between the adjacent layers, and hence increased interfacial thermal resistance. However, if the total length of the superlattice nanowire is fixed, reducing the period length will lead to decreased effective thermal conductivity due to the increased number of interfaces. Finally, it is found that the interfacial thermal resistance decreases as the reference temperature increases, which might be due to the inelastic interface scattering.

INTRODUCTION

Semiconductor superlattices (SL) are of great interest due to their potential applications in thermoelectric and optoelectronic devices [1,2]. Superlattice structures provide the possibility of decreasing materials' thermal conductivity while retaining their electrical conductivity, thus achieving a high thermoelectric figure-of-merit and improving the performance of thermoelectric devices. A large amount of experimental and theoretical work [3-8] has been carried out to study the effects of lattice period and interface on the thermal conductivity of various kinds of superlattice films. Results showed that the superlattice may have a much lower thermal conductivity than the value for each of the two materials composing the superlattice structure along both the in-plane and the cross-plane directions. Different mechanisms have been proposed to explain the reduction of the thermal conductivity, including interface phonon scattering due to acoustic impedance mismatch, phonon scattering by crystal imperfections at the interface, phonon spectrum mismatch, and mini-band formation. However, quantitative analysis of the relative importance of

[a] yunfeichen@yahoo.com

these different mechanisms has not been completed yet and it is not clear which mechanism contributes most to the reduction of the thermal conductivity under different conditions. Experimental results [6,7] indicate that as the period of the superlattice decreases, the thermal conductivity along the cross-plane direction also decreases, and for very short period superlattice, its thermal conductivity could even fall below the alloy limit, i.e. if the two materials mixed homogeneously into an alloy. The in-plane thermal conductivity follows a similar pattern but it jumps to higher values for some very short period superlattice [8]. This phenomenon cannot be explained solely by diffuse mismatch theory about phonon scattering at the interface. Other mechanisms such as acoustic impedance mismatch, mini-band formation or phonon spectrum mismatch have to be taken into account.

Theoretically, lattice dynamics and particle transport models are usually used to study the thermal conductivity of superlattice structures. Some recent lattice dynamics work was carried out by Hyldgaard and Mahan [9] and Tamura and Tanaka [10]. In their work, a simple cubic lattice model [9] and a face-centered cubic model [10] were used to calculate the group velocity of acoustic phonons in the cross-plane direction. Their results suggested that reduction of the phonon group velocity in superlattices could lead to a reduced thermal conductivity. Considering their lattice models were too simple to provide details of phonon dispersion spectra, Kiselev *et al*. [11] used a diatomic unit cell model to simulate the dispersion spectra of the Si/Ge superlattice. Due to the large mass of Ge atoms in comparison to Si, the most probable acoustic phonons in Si layers at room temperature have no counterpart in the phonon spectra of the Ge layers. In other words, a phonon at a given frequency in the Si layer may not be able to proceed into the Ge layer without scattering with, or into, one or more phonons of different frequency. This leads to highly efficient trapping of high-energy phonons in the Si layer and a drastic reduction of the superlattice thermal conductivity. Although qualitative agreement can be obtained through lattice dynamics, it is difficult to compare those results quantitatively with experimental results for different materials under different temperatures due to the fact that lattice dynamics can only model very simple systems. The particle transport model treats phonons as individual particles and solves the Boltzmann transport equation (BTE) to study the phonon transport in microstructures. Simkin and Mahan [12] showed that for layers thinner than the mean free path (mfp) of phonons, the wave aspect of phonons must be taken into account and wave theory must be applied, while for layers thicker than the mfp of phonons, the particle treatment of phonons was acceptable and BTE could be used to study the phonon transport. The first study on the thermal conductivity of superlattices was carried out by Ren and Dow [13]. They modeled the thermal conductivity of ideal superlattice by combining the BTE with a quantum mechanical treatment of the additional scattering process caused by the mini-bands. However, their predicted results could not match the experimental data. Based on the BTE and the assumption of partially specular and partially diffuse boundary scattering, some interesting results were obtained by G. Chen *et al*. [14-17] for superlattice thermal conductivity along both in-plane and cross-plane directions. In his model the reduction of the superlattice thermal conductivity was mainly attributed to diffuse scattering at the interface.

Because some assumptions must be introduced to get closed form solutions, the theoretical results usually deviate significantly from the experimental data and sometimes the thermal conductivity reduction mechanisms cannot be readily explained from those theoretical studies. Classical Molecular Dynamics (MD) simulation provides an alternative approach to investigate heat transport in nanostrucutres. Given the interaction potential between atoms, the force acting on each atom can be calculated. Based on Newton's second law, the motion of a large number of atoms can be described. Without any further assumptions, statistical physical properties can be derived from the ensemble of atoms. In particular, if the size of the nanostructure is smaller than the phonon mean free path, it is questionable to use the BTE to describe phonon transport, while MD can be conveniently used to analyze the effects of size confinement on lattice thermal conductivities. Volz *et al.* [18] demonstrated by MD simulation that Si nanowire thermal conductivity could be two orders of magnitude smaller than the corresponding bulk value and they further argued that by adjusting the specularity parameter, results from the solution of the BTE could fit their MD simulation. Liang *et al*. [19] applied MD simulation to investigate the effects of atomic mass ratio in the alternating layers of a superlattice on the lattice thermal conductivity. Their results indicated that the thermal conductivity has a minimum value for some specific atomic mass ratio. Abramson *et al*. [20] studied the effects of interface number and elastic strain on the lattice thermal conductivity of Kr/Ar superlattices with MD simulation. It was argued that increase of the interface number per unit length does not necessarily result in decreased lattice thermal conductivity from their simulation results. Daly et al [21,22] reported MD simulation of a classical face centered cubic (FCC) lattice model to study the effects of interface roughness and isotope scattering on thermal conductivities. Simulation results predicted the similar trends for the lattice thermal conductivities of GaAs/AlAs superlattice along both in-plane and cross-plane directions compared with the experimental data [23]. In their model, it was also demonstrated that the lattice thermal conductivity of GaAs/AlAs superlattice had a minium value with different layer thickness. This conclusion supported the hypothesis that zone folding was the dominant effect on lattice thermal conductivity in the short period superlattice. However, it should be noted that no lattice mismatch between the alternative materials of the superlattice was considered in their model. Volz [24] introduced the conjugate gradient method to minimize the potential energy of Si/Ge superlattices in order to relax the elastic strain on the alternating layers. Simulation results predicted an increasing trend of the superlattice thermal conductivity with the layer thickness.

Recently, experimental investigation on the thermal conductivity of Si and Si/SiGe superlattice nanowires has been carried out [25,26]. Their results showed that for Si nanowires, the thermal conductivity could be greatly reduced compared with that of bulk Si because of the strong nanowire boundary scattering. For Si/SiGe nanowires, the thermal conductivity was below that of the 2 dimensional Si/SiGe superlattice films, which was ascribed to the additional scattering mechanism

provided by the nanowire boundary. In this paper, we apply molecular dynamics to study the lattice thermal conductivity of Kr/Ar superlattice nanowires in order to investigate the effects of interface scattering, nanowire boundary scattering, and period length.

Theoretical Model and Analysis

Nonequilibrium molecular dynamics (NEMD) was used to calculate the lattice thermal conductivities of solid Ar and Kr/Ar superlattice nanowires in the present study. The Lennard-Jones (L-J) potential was used to represent the interaction between two particles,

$$V_{ij}(r) = 4e_{ij}\left\{\left(\frac{\sigma_{ij}}{r}\right)^{12} - \left(\frac{\sigma_{ij}}{r}\right)^{6}\right\} \qquad (1)$$

where subscripts i and j stand for either argon or krypton particles, e_{ij} and σ_{ij} represent the energy and length scale of the potential, and r denotes the distance between the two particles. Table I gives the selected parameters and the simulation domain for the Kr/Ar superlattice nanowire is shown in Figure 1.

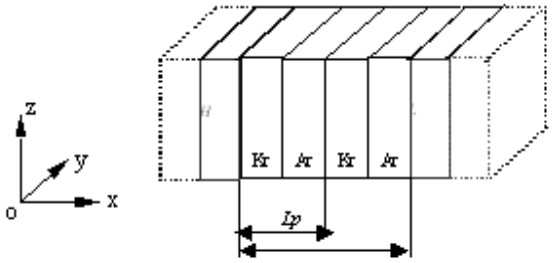

Figure 1. Physical model of Kr/Ar superlattice nanowire

The simulation domain consisted of a hot bath with a high constant temperature T_H, a cold bath with a low constant temperature T_L and alternating Kr/Ar layers. Constant heat flux was added to the hot bath and the same amount of heat flux was subtracted from the cold bath at the same time. In this way, heat flux was introduced into the simulation domain and a temperature gradient was set up along the heat flux direction. From the heat flux J and the temperature gradient, the thermal conductivity of the nanowires can be calculated from the Fourier law

$$K = \frac{-J}{A\nabla T} \qquad (2)$$

where A is the cross sectional area and ∇T is the temperature gradient. The temperature gradient can be obtained according to the equation

$$\nabla T = \frac{T_H - T_L}{L_p \times N} \qquad (3)$$

where L_p and N are the length and the number of periods for the superlattice nanowire shown in Figure 1. T_H and T_L temperatures of the bath atoms in contact with either side of the nanowire. Phonon scattering at the interfaces between the hot and cold baths and the superlattice structure leads to temperature jumps between the thermal bath layers nearest the nanowire and the first adjacent layer of the nanowire [27,28], which results in a smaller temperature gradient within the wire than that imposed externally. In our simulation, Kr atoms were selected to form the hot bath and Ar atoms were selected as the cold bath material in order to minimize the interfacial thermal resistance on either side. Fixed boundary conditions on the outer surface of the nanowire were introduced to avoid evaporation from the nanowire domain during the simulation process. In the fixed boundary regions, the atoms were fixed in their equilibrium positions. They interacted with the atoms in the nanowire through the L-J potential. The parameters are listed in Table I[27]. In Figure 1 the fixed boundary regions in the x direction are depicted by the dashed lines. The thickness of the fixed boundary region was set as 1 unit cell (*UC*). It has been shown [18] that for Si nanowires, the difference between fixed boundary condition and free boundary condition was less than 10%. According to Lukes *et al.* [27], two important criteria for the simulation are that the effective thermal flux in each atomic layer is nearly the same as that imposed externally, and that the temperature profiles are reasonably close to linear. The profiles should not be expected to be completely linear, since the thermal conductivity is temperature dependent. In order to satisfy the two criteria, computation time should be selected as long as possible for the system to reach steady state. In this paper, to avoid undue computational burden, values roughly 20 times of the characteristic diffusion time were found sufficient to satisfy the criteria. For the thermal conductivity simulations reported here, the values of the effective thermal flux were all within four percent of the imposed flux and the temperature profiles were reasonably linear.

Table I Simulation parameters

Variables		Parameters
Kr-Kr	ε_1 (J)	2.25×10^{-21}
	σ_1 (m)	3.65×10^{-10}
	Lattice constant A_1 (m)	5.69×10^{-10}
	Atom mass M_1 (Kg)	1.39×10^{-25}
Ar-Ar	ε_2 (J)	1.67×10^{-21}
	σ_2 (m)	3.4×10^{-10}
	Lattice constant A_2 (m)	5.3×10^{-10}
	Atom mass M_2 (Kg)	6.63×10^{-26}
Kr-Ar	ε_{12} (J)	$\sqrt{\varepsilon_1\varepsilon_2}$
	σ_{12} (m)	$(\sigma_1+\sigma_2)/2$

Local temperature calculation is another issue to be concerned in MD simulation, which relates to the size of the region over which temperature is defined. To define a local temperature, local thermodynamic equilibrium must be set up, which means that the temperature must be defined over a region with characteristic length larger than the phonon mean free path. However, it has been shown that for classical MD simulation, local temperature can be defined for each layer of

atoms as long as there are enough atoms in each layer [30]. In this paper, T_p in the profile was evaluated from the equation

$$T_p = m_a \sum_{i=1}^{N_p} v_i^2 \Big/ 3N_p k_B \qquad (4)$$

where m_a, N_p are the mass and the number of atoms in a local plane, v_i is the velocity of each atom, and k_B is the Boltzmann constant. The criteria for Equation (4) to be valid are that local thermodynamic equilibrium is established in each layer, and the simulation temperature is above the Debye temperature of the material so that the heat capacity is temperature independent. According to Hafskjold [30], at least 30 atoms are needed in each layer in order to reach local equilibrium and to define an instantaneous temperature. So for a superlattice nanowire with a square cross section, the width of the cross section should be up to at least 4 *UC*. On the other hand, Lukes *et al.* [27] demonstrated that prolonging the simulation time was more efficient for a system to reach equilibrium compared with increasing the number of atoms in the simulation system. So in our simulation, the lower limit of the cross sectional area of the superlattice nanowires was selected as $4UC \times 4UC$. As the simulation temperature in this paper was below the Debye temperatures of Kr and Ar (72K, 92K respectively), quantum modification should be introduced to correct both the MD temperature and the thermal conductivity. However, it has been suggested [31] that the classical MD model could give acceptable prediction for lattice thermal conductivity as long as the temperature is higher than one-fourth of the Debye temperature. Since the reference temperature in our simulation system is above one-fourth of the Debye temperature for both Kr and Ar, for simplicity, we still used Equation (4) to estimate the local temperature.

Temperature discontinuity appeared in the temperature profile at interfaces between Kr and Ar layers along the superlattice nanowires, which was caused by the interfacial thermal resistance. The interfacial thermal resistance can be calculated from the following equation [32]

$$R_{\text{int}} = \frac{\Delta T}{J / A} \qquad (5)$$

where A is the cross sectional area, ΔT is the temperature discontinuity at the interface and J is the heat flux. The interfacial thermal resistance depends on the number of the phonons incident on the interface, the energy carried by each phonon and the probability that each phonon is transmitted across the interface. Two limiting models have been proposed to describe phonon transport across an interface: the acoustic mismatch model, which assumes specular reflection of phonons at the interface, and the diffuse mismatch model, which assumes that all phonons incident on the interface will be diffusely scattered. However, it is difficult to argue if the interfacial thermal resistance can be calculated from these two models because of the strong assumptions made in these two theories. On the other hand, in MD simulation, the interfacial thermal resistance can be readily calculated from Equation (5) according to the classical definition of interfacial thermal resistance. The total thermal resistance along the nanowire can be described as

$$R_{tot} = n * R_{\text{int}} + N * (R_A + R_B) \qquad (6)$$

where n is the number of the interface, N is the number of periods and $n = 2 * N - 1$. R_A, R_B are the thermal resistance of each Ar and Kr layer, respectively. Equation (6) is only an approximate expression for the total thermal resistance. In fact, due to the difference of the reference temperature in different layers along the superlattice nanowire, the thermal resistances R_A, R_B should not be exactly the same for different sections. Assuming that R_A, R_B are the same along the whole nanowire, the effective thermal conductivity of the superlattice nanowire can be approximated as

$$K_{eff} = \frac{L_p}{R_A + R_B + 2R_{\text{int}} - R_{\text{int}} / N} \qquad (7)$$

As we know, under atmospheric pressure, for an interface between two bulk materials, if there is no interface imperfection, the interfacial thermal resistance only depends on temperature and the materials that constitute the interface. Once the materials and the temperature are determined, the interfacial thermal resistance should be a constant. Thus, from Equation (7), it can be concluded that the effective thermal conductivity of superlattice nanowire will depend on the length and number of periods. It predicts that the thermal conductivity of the superlattice nanowire increases with the period length. However, for superlattice nanowires, due to the fact that the period length may be less than the phonon mean free path, the thermal resistance in the alternating layers and the interfacial thermal resistance are all layer thickness dependent, so the relation between the effective thermal conductivity and the period length might be nonlinear.

Simulation results and discussion

Effect of the number of interfaces

NEMD was used to predict lattice thermal conductivities of pure Ar and Kr/Ar superlattice nanowires. Figure 2 shows the thermal conductivities of Ar and Kr/Ar superlattice nanowires versus nanowire length for a fixed period length of 8 *UC*. For the Kr/Ar superlattice nanowire, one period is composed of two layers and the thickness of each layer is 4 *UC*. The total length of the Ar nanowire was chosen to be the same as that of the Kr/Ar superlattice nanowire. Also, the two kinds of nanowires are of the same cross sectional area as $4UC \times 4UC$. The temperatures in the hot bath and the cold bath are 50 K and 10 K, respectively, and the reference temperature is 30 K. Figure 2 shows that the thermal conductivity of the Kr/Ar nanowire is only about one-third of that of the Ar nanowire, which we believe is due to the additional interface scattering in the Kr/Ar superlattice nanowire. For Ar nanowire, its thermal conductivity increases as the length of the nanowire increases up to 40 *UC*. We believe that this is due to the scattering from the heat source and heat sink. If the length of the simulation domain is shorter than the phonon mean free path, then the nanowire thermal conductivity should be length dependent, i.e. the thermal conductivity increases with the length of the simulation domain. The phonon mean free path for Ar [31] is estimated to be approximately 5 nm (10~16 *UC* for Ar and Kr) at 30 K. However, low frequency phonons have longer mean free paths while high frequency phonons have shorter mean free paths,

which means that even for a system of a length longer than the phonon mean free path, the effects of phonon scattering at the heat source and heat sink may still have some effect on the total thermal conductivity. In our calculation, the thermal conductivity of Ar nanowire increases with the nanowire length until the length exceeds 40 *UC*, which we think comes from the scattering of long wavelength phonons at the heat source and heat sink. Typically for simulations on bulk materials one should not see a size dependence and for those cases size effects would be an unphysical artifact. However for materials with characteristic dimensions on or below the order of a phonon mean free path, there will be a size dependence and it is a true, physical effect [27]. It is attributed to the length of the nanowire is smaller than the phonon mean free path. Thermal conductivity in that case is not intrinsic but is dominated by boundary effects. Nonetheless, this size dependent phenomenon cannot be observed for Kr/Ar superlattice nanowire, as shown in Figure 2. With the increase of nanowire length, the thermal conductivities of Kr/Ar superlattice nanowires remain almost constant and a very slight decreasing trend appears when the period number exceeds 5. The reason might be that the effects of phonon scattering at the boundaries of the hot and cold baths are masked by the interface scattering. The effects of phonon scattering on the heat source and heat sink boundaries play the same role as the interface scattering so for superlattice nanowires, the data of the thermal conductivities for different length of the nanowire superlattice seem to be consistent with formula (7), i.e. for a fixed period length superlattice nanowire, its thermal conductivity keeps constant.

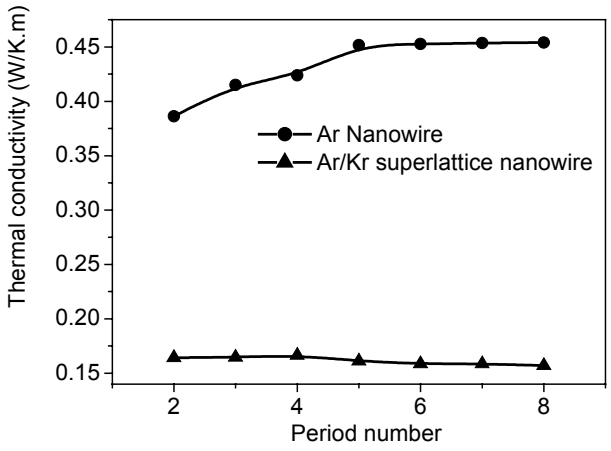

Figure 2.Thermal conductivities of Ar and Kr/Ar superlattice nanowires

Effect of period length on the thermal conductivity and the interfacial thermal resistance

In order to study the effects of period length, Kr/Ar superlattice and superlattice nanowires of different period length were investigated with a fixed total length of 48 UC and a cross sectional area of $4UC \times 4UC$. Figure 3 gives thermal conductivity versus period length, which reveals the effects of the interface and nanowire boundary on the lattice thermal conductivity. For nanowires of fixed total length, the lattice thermal conductivity increases with the period length because fewer interfaces are present in the longer period superlattice nanowire. In addition, the interfacial thermal resistance is not a constant as the period length changes. It increases as the period length increases, as shown in Figure 4. This phenomenon is attributed to the interface strain effects on phonon transport [20]. The atomic spacing on either side of the interface tends to either slightly contract (for Kr atoms) or expand (for Ar atoms) to align with adjacent atoms because of the lattice mismatch between these two materials. For short period superlattice nanowires, the elastic strain causes the lattice in the adjacent layers to match better with each other, which poses less resistance to phonon transport. The difference of elastic strain for different period length is shown in Figure 5. The cross sectional areas for the two nanowires are $5.19nm^2$ and their period lengths are 4.4 nm and 13.2 nm respectively. Two and three periods were simulated for the 13.2 nm and 4.4 nm period length nanowires, respectively, so the nanowires are labeled as $2 \times 13.2nm \times 5.19nm^2$, $3 \times 4.4nm \times 5.19nm^2$, The two dashed lines labeled Kr and Ar stand for the distance between two neighboring atomic planes along the x axis for pure Kr and pure Ar, respectively. For the longer period nanowire, the atomic planes far away from the interface tend to maintain the equilibrium spacing found in the pure material. For the shorter period nanowire, however, most of the atoms in the two layers deviate from their equilibrium spacing, as shown in Figure 5. We believe that as the period length increases, the acoustic impedance mismatch between the two different material layers increases, which causes the larger interfacial thermal resistance as shown in Figure 4. However, because the total length of the nanowire is fixed, the ratio of the total interface resistance to the total effective thermal resistance decreases for increasing period length. This is due to the fact that the number of interfaces is reduced for longer period superlattice nanowires if the total length of the nanowire is fixed.

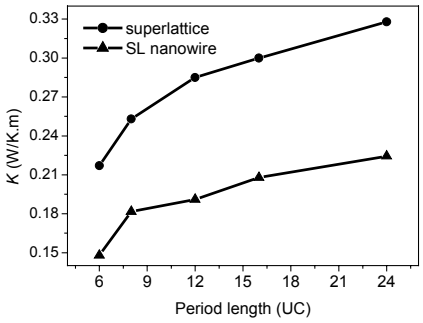

Figure 3. Thermal conductivities of Kr/Ar superlattice and superlattice nanowires.

Figure 3 also gives the thermal conductivity of a Kr/Ar superlattice film in order to compare the effects of cross sectional area on the thermal transport. The period length for the superlattice is the same as that of Kr/Ar superlattice nanowires. Periodic boundary conditions were imposed in y and z directions to stand for infinite cross sectional area. Simulation results show that the thermal conductivity of superlattice films is much higher than that of superlattice nanowires for the same period length, which is consistent as the

experimental observations [26]. This means that in addition to the interface scattering in superlattice nanowire, the nanowire boundary scattering pose significant resistance to the phonon transport.

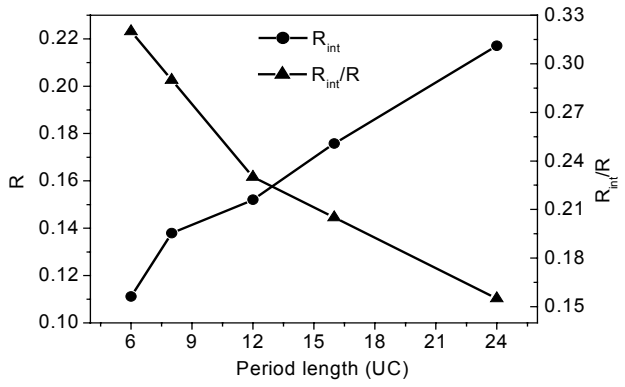

Figure 4. Interfacial thermal resistance of superlattice nanowire

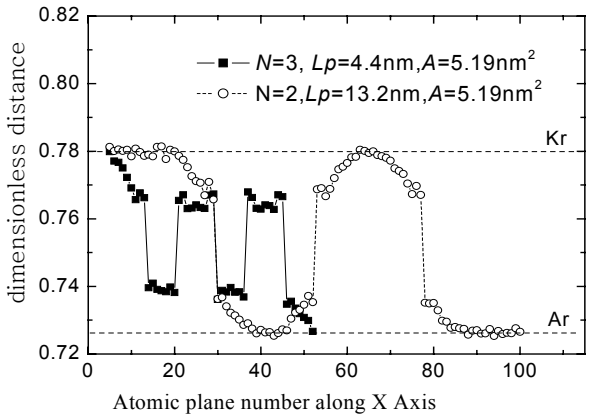

Figure 5. Elastic strain in Kr/Ar superlattice nanowires

Effects of cross sectional area on the thermal conductivity and the interfacial thermal resistance

At low temperature, thermal conductivity increases with the sample size due to the fact that phonon-boundary scattering dominates the thermal resistance. For larger cross section, the probability of phonon-boundary scattering reduces, which leads to higher lattice thermal conductivity. To explore the effects of different cross sectional area on the thermal conductivity of superlattice nanowires, we simulated thermal transport in nanowires of different cross sectional area as $4UC \times 4UC$, $5UC \times 5UC$, $6UC \times 6UC$ and $7UC \times 7UC$. To save computational time, the total length of the nanowire was chosen as 24 *UC,* the period length as 8*UC,* and the thickness of each layer as 4 *UC*. The simulation results are shown in Figure 6. It can be seen that the thermal conductivity increases nearly linearly with the size of the cross section. If we assume constant specific heat for all four nanowires, kinetic theory predicts that the thermal conductivity is proportional to the phonon mean free path. The equivalent phonon mean free path can be written as

$$\frac{1}{l} = \frac{1}{l_{phonon}} + \frac{1}{l_{interface}} + \frac{1}{l_{boundary}} \qquad (8)$$

where the subscripts 'phonon', 'interface' and 'boundary' stand for the effective phonon mean free path determined by the three phonon scattering process, the interface scattering, and nanowire boundary scattering, which is related to the cross section size. If we do not take into account the modification of the phonon dispersion relation due to the different diameters of the nanowires, the phonon mean free path due to anharmonic scattering can be approximated as constant. From equation (8), it can be deduced that the effective thermal resistance of the nanowire decreases for increasing cross section, which is confirmed by the results shown in Figure 6. Figure 7 shows that for superlattice nanowires, the ratio of the interfacial thermal resistance to the total thermal resistance increases as the cross sectional area increases. If the cross sectional area increased to infinity, i.e. the superlattice nanowire becomes the superlattice film, the ratio increased to 42%.

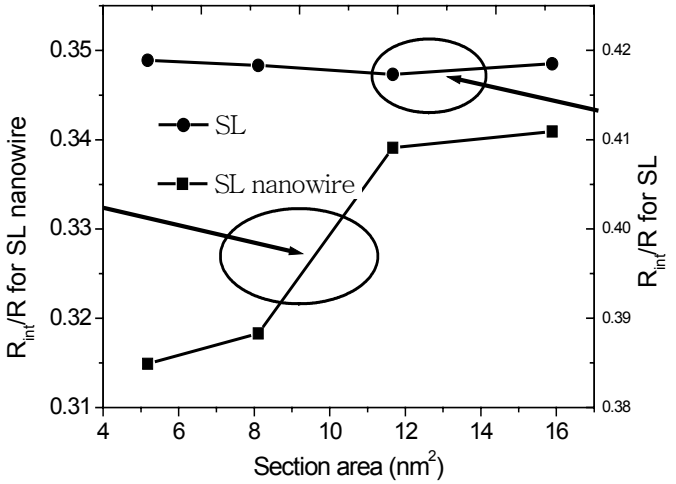

Figure 6. Thermal conductivity of superlattice and superlattice nanowire

For Kr/Ar superlattice films shown in Figure 6 and Figure 7, the period length and period number are the same as that of the superlattice nanowires. The difference between the superlattice films of different simulation domain is only marginal due to the periodic boundary conditions for superlattice films. The value of the thermal conductivity for superlattice films is the upper limit of the thermal conductivity for superlattice nanowires. This is also true for the ratio of the interface resistance to the total thermal resistance, as shown in Figure 7. Considering the minor difference among the nanowire's diameter for the four types of nanowires, any resulting differences in dispersion relation will be slight so the change of the phonon dispersion relations among the nanowires is neglected [34,35]. The reduced influence of boundary scattering processes for the thicker nanowires is the main reason that the value of thermal conductivity increases with the cross sectional area.

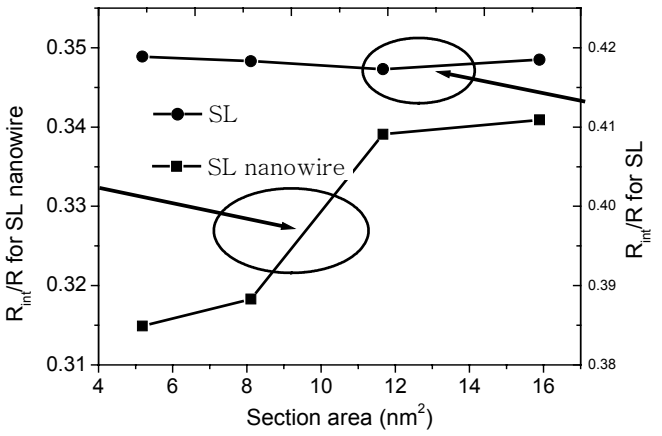

Figure 7. Interfacial thermal resistance of superlattice and superlattice nanowires.

The dependence of interfacial thermal resistance on temperature

The total thermal resistance of a superlattice nanowire equals the sum of the thermal resistance in each layer and the interfacial thermal resistance. From both the acoustic mismatch model and the diffuse mismatch model, at very low temperature, the interfacial thermal resistance decreases with temperature at a rate proportional to T^3, due to the temperature dependence of specific heat. As the temperature rises, the specific heat approaches a constant value, so the interfacial thermal resistance also approaches a constant value. Figure 8 plots the interfacial thermal resistance and the thermal conductivity of superlattice nanowires versus temperature, which shows that as the temperature increases, both the interfacial thermal resistance and the nanowire thermal conductivity decrease in the temperature range of 35 to 55 K. The reason for the thermal conductivity reduction can be ascribed to the increased thermal resistance of each layer due to phonon-phonon scattering. However, the reason for the interfacial thermal resistance decrease is not fully understood. From the acoustic mismatch model, the thermal boundary resistance can be approximated as $(\frac{1}{4}Cv_s\alpha)^{-1}$, where, C, v_s, and are the specific heat, the Debye phonon group velocity, and the averaged phonon transmission probability. The Debye phonon group velocity can be regarded as a constant. The phonon transmission probability is typically assumed in the literature to be independent of temperature [32]. The above equation predicts that the thermal boundary resistance is independent of temperature. The decrease of the interfacial thermal resistance cannot be derived from the diffuse mismatch model either. One possible reason might be that inelastic scattering occurs at the interface [32]. At higher temperature, the high frequency phonons might break into two or more low frequency phonons, which will be predominantly transmitted. This inelastic scattering process leads to higher phonon transmission probabilities, thus the interfacial thermal resistance decreases.

Conclusion

In summary, the lattice thermal conductivity of Ar nanowires and Kr/Ar nanowires were studied by nonequilibrium molecular dynamics. The interfacial thermal resistance in the Kr/Ar nanowires contributes significantly to the thermal resistance and results in a lattice thermal conductivity that is only one third of that of pure Ar nanowires. Interfacial thermal resistance increases with the length of the superlattice period for the Kr/Ar superlattice nanowires, which is attributed to increased acoustic impedance mismatch between adjacent layers for long period nanowires. For short period nanowires, the acoustic impedance in the alternating layers beside the interface matches better due to elastic strain throughout each layer. The phonons can pass through the interface more easily, which results in smaller interfacial thermal resistance. On the other hand, for longer period superlattice nanowires, the atoms located far away from the interface maintain their pure crystalline lattice positions so that the strain is localized near the interface. It is more difficult for phonons to pass through the interface due to the larger acoustic impedance mismatch between the two layers.

If the total length of the superlattice nanowire is fixed, increasing the interface number per unit length will lead to decreased interfacial thermal resistance. However, the effective thermal conductivity for the superlattice nanowire decreases due to the fact that the number of interfaces increases. Nanowire boundary scattering also contributes to the total thermal resistance. Increasing the cross sectional area of superlattice nanowires leads to higher thermal conductivity. The ratio of the interfacial thermal resistance increases with the cross sectional area, and as an upper limit, the ratio of the interfacial thermal resistance to the total thermal resistance reaches 42% for Kr/Ar superlattice films. It is also found that the interfacial thermal resistance decreases with the temperature, which might be explained by inelastic phonon scattering at the interface.

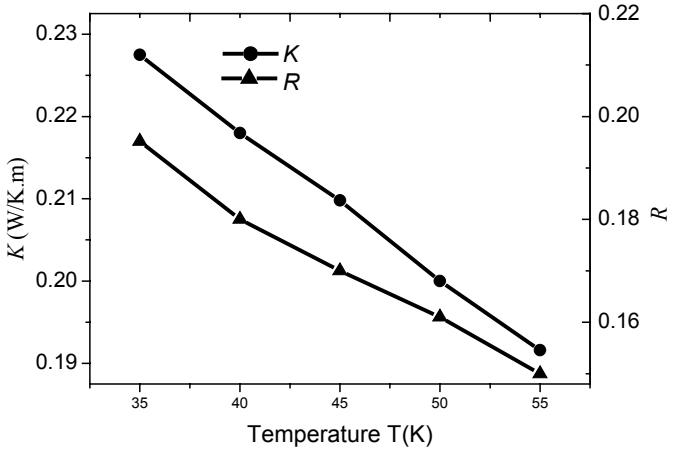

Figure 8. Thermal conductivity and interfacial thermal resistance of Kr/Ar superlattice nanowire

Acknowledgment:

Y.C would like to acknowledge the financial support of the Chinese Natural Science Foundation (Project No.

50276011,50275026) and the 863 High Technology Program (Project No. 2003AA404160).

Reference:

1. X. Fan, G. Zeng, C. LaBounty, J. Bowers, E. Croke, C. Ahn, S. Huxtable, A. Majumdar, and A. Shakouri, Appl. Phys. Lett. **78** (2001), 1580.
2. M. R. Kitchin, M. J. Shaw, E. Corbin, J. P. Hagon, M. Jaros, Physical Review B **61** (2000) , 8375.
3. T. Yao, Appl. Phys. Lett. **51** (1987) , 1798.
4. G. Chen, C.L. Tien, X. Wu, and J. S. Smith, J. Heat Trans. **116** (1994) , 325.
5. X. Y. Yu, G. Chen, A. Verma, and J. S. Smith, Appl. Phys. Lett. **67** (1995) , 3554.
6. S.–M. Lee, D. Cahill, and R. Venkatasubramanian, Appl. Phys. Lett. **70** (1997) , 2957.
7. W.S. Capinski and H.J. Maris, Physica B **219** (1996) , 699.
8. S. T. Huxtable, A.R. Abramson, C-L, Tien, Arun Majumdar, Appl. Phys. Lett. 80 (2002) , 1737.
9. P. Hyldgaad and G.D. Mahan, Phys. Rev. B **56** (1997) , 10754.
10. S. Tamura and Y. Tanaka and H.J.Maris, Phys. Rev. B **60** (1999) , 2627.
11. A. A. Kiselev, K. W. Kim, and M.A. Stroscio, Phys. Rev. B **62** (2000) , 6896.
12. M. V. Simkin and G. D. Mahan, Phys. Rev. Lett. **84** (2000), 927.
13. S. Y. Ren and J. D. Dow, Phys. Rev. B **25** (1982), 3750.
14. G. Chen, J. Heat Trans. **119** (1997) , 220.
15. G. Chen, Phys. Rev. B **57** (1998) , 14958.
16. G. Chen and M. Neagu, Appl. Phys. Lett. **71** (1997), 2761.
17. G. Chen, J. Heat Trans. **119** (1996), 220.
18. S. Volz and G. Chen, Appl. Phys. Lett. **75** (1999), 2056.
19. X. G. Liang, B. Shi, Materials Sci. Eng. A. **292** (2000) , 198.
20. A. R. Abramson, C.-L. Tien, and A. Majumdar, J. Heat Trans. **124** (2002) **,** 963.
21. B.C. Daly, H.J.Maris, K.Imamura and S. Tamura, Phys. Rev. B,66 (2002) , 024301.
22. B.C. Daly, H.J.Maris, K.Imamura and S. Tamura, Phys. Rev. B,67 (2003) , 033308.
23. W. S. Capinski, H. J. Maris, T. Ruf, M. Cardona, K. Ploog, and D.S. Katzer, Phys. Rev.B, 59 (1999) ,8105.
24. S. Volz, J.B. Saulnier, G. Chen, P. Beauchamp, Microelectronics Journal, 31, 815, 2000.
25. D. Li, Y. Wu, P. Kim, L. Shi, P. Yang, and A. Majumdar, Appl. Phys. Lett. 83 (2003),2934.
26. D. Li, Y. Wu, R. Fan, P. Yang, and A. Majumdar, Appl. Phys. Lett. 83 (2003),3186.
27. J. R. Lukes, D. Li, X.-G. Liang, and C.-L. Tien, J. Heat Trans. **122** (2000) , 536.
28. P. K. Schelling, S. R. Phillpot, and P. Keblinski, Phys. Rev. B. **65** (2002) , 144306.
29. H. B. G. Casimir, Physica **5** (1938) , 595.
30. B. Hafskjold and S.K. Ratkje. J. Statistical Phys. **78** (1995) , 463.
31. H. Kaburaki, J. Li, and S. Yip, Materials Research Society Symposium Proceedings **538** (1998) , 503.
32. E. T. Swartz and R.O. Pohl, Rev. Mod. Phys. **61** (1989) , 605.
33. S. Volz, J.-B. Saulnier, M. Lallemand, B. Perrin, P. Depondt, and M. Mareschal, Phys. Rev. B **54** (1996) , 340.
34. C. Dames and G. Chen, Journal of Applied Physics, 95(2),682,2004.
35. J.Zou and A. Balandin, Journal of Applied Physics, 89(5),2932,2001.